

# Distribution of artificial radionuclides in particle-size soil fractions

---

Received: 4 October 2025

Accepted: 2 February 2026

Published online: 10 February 2026

Cite this article as: Kunduzbayeva A., Kabdyrakova A., Mendubayev A. *et al.* Distribution of artificial radionuclides in particle-size soil fractions. *Sci Rep* (2026). <https://doi.org/10.1038/s41598-026-39072-8>

Assiya Kunduzbayeva, Alua Kabdyrakova, Ayan Mendubayev, Andrey Panitskiy, Natalya Larionova & Viktor Baklanov

---

We are providing an unedited version of this manuscript to give early access to its findings. Before final publication, the manuscript will undergo further editing. Please note there may be errors present which affect the content, and all legal disclaimers apply.

If this paper is publishing under a Transparent Peer Review model then Peer Review reports will publish with the final article.

ARTICLE IN PRESS

## DISTRIBUTION OF ARTIFICIAL RADIONUCLIDES IN PARTICLE-SIZE SOIL FRACTIONS

Assiya Kunduzbayeva<sup>a</sup> (corresponding author,  
kunduzbaeva@nnc.kz), Alua Kabdyrakova<sup>b</sup>, Ayan  
Mendubayev<sup>a</sup>, Andrey Panitskiy<sup>a</sup>, Natalya Larionova<sup>a</sup>,  
Viktor Baklanov<sup>c</sup>

<sup>a</sup> Branch office 'Institute of Radiation Safety and Ecology' of the NNC RK,  
Kurchatov t., Kazakhstan

<sup>b</sup> National Nuclear Center, Kurchatov t., Kazakhstan

<sup>c</sup> Branch office 'Institute of Atomic Energy' of the NNC RK, Kurchatov t.,  
Kazakhstan

**Keywords:** radioactively contaminated soils, <sup>137</sup>Cs, <sup>241</sup>Am, radioactive waste, Semipalatinsk Nuclear Test Site, fractional separation.

### Abstract

Experimental studies were carried out to evaluate the efficiency of fractional separation of radioactively contaminated soils with respect to gamma-emitting <sup>137</sup>Cs and <sup>241</sup>Am. The research was conducted using samples from radiation-hazardous objects (craters) located at the Semipalatinsk Nuclear Test Site and resulted from ground and excavation nuclear explosions. The most appropriate parameter reflecting the distribution pattern of artificial radionuclides <sup>137</sup>Cs and <sup>241</sup>Am across soil fractions resulting from nuclear blasts is the enrichment factor (Ef). Dry fractional separation can be recommended as a promising method for the decontamination of soils contaminated with cesium.

### Introduction

The widespread use of nuclear energy and radioactive materials in industry, medicine, agriculture, scientific research, and education, as well as activities involving the treatment of mineral ores or other materials containing naturally occurring radionuclides, is associated with the generation of radioactive waste [1]. Radioactive waste, as a source of ionizing radiation, can pose a hazard to human health and the environment.

The issue of decontaminating radioactively contaminated soils (RCS) is particularly relevant in the context of decommissioning nuclear facilities and nuclear legacy objects. These are areas were contaminated due to the technological limitations of early nuclear industry development and poor radioactive waste (RW) management practices, as well as due to nuclear accidents and incidents [2, 3].

The most widely used approach for remediating contaminated areas is the extraction and disposal of radioactive soil for long-term controlled

storage. However, when dealing with large-scale contaminated sites, this approach is not optimal due to the need to manage large volumes of contaminated material and the associated high material and financial costs, including transportation [4]. An alternative to the excavation and disposal of all radioactively contaminated soil (RCS) is partial decontamination—reducing the activity concentration level to within acceptable limits set by hygienic standards [5].

A qualitative composition of radioactive contamination generated by a nuclear explosion was determined by fission fragments, unreacted components of nuclear fuel and by neutron activation products of construction materials in a nuclear explosive device and environmental elements [6]. During ground (GTE) and underground explosions with soil ejection (excavation explosions) (ENE, ETE), a prevailing generation mechanism of radioactive particles is the sorption of radionuclides by the aggregate of polydisperse initially melted ground particles.

The ground explosions produce particles in a broad range of physical and chemical characteristics. In the vicinity of an explosion, large (as big as several millimeters in diameter) spherical particles (type 1 particles) generally fall out. By the chemical composition, particles of this type are close to ground, have a volume pattern of debris distribution. In the zone of depositions from a ground nuclear explosion, irregularly shaped surface-sintered particles can also be found (type 2 particles). Their concentration ratio rises as the distance from the ground zero increases. The debris in these particles is solely concentrated in the sintered layer. In view of low activity values, the role of this type of particles is marginal in the radioactive contamination of the ground. Radioactive particles during explosions with soil ejection are divided into two types. Melted (slag) particles form the basis of the fallout from an explosion cloud and are irregularly (arbitrarily) or regularly shaped (spherical, drop-shaped, dumbbell-shaped etc.) with a vitreous structure. Slag particles are highly brittle, the debris is distributed virtually uniformly by volume and their total activity concentration is the highest. Type 2 particles are shattered (crystalline), which form the basis of a base surge depositions. The size range is essentially narrower than that of melt particles, and the debris is only concentrated on the surface. The

activity concentration of crystalline particles is well below that of melt particles [7].

The generation of radioactive particles is also affected by fractionation interrelated to explosion conditions, thermophysical and nuclear-physical characteristics of elements, whose shapes contain debris while radioactive particles are generated. One of the important features of a fractionation effect is that the nearby fallout from a ground and underground excavation nuclear explosion is enriched with nuclides of refractory chemical and depleted with nuclides of readily fusible chemical elements and nuclides with long-lived volatile and gaseous precursors. A far zone of the fallout 'plume' has an opposite picture [8].

The goal of this study is to evaluate the decontamination efficiency of radioactively contaminated waste using the particle-size fractionation method, based on case studies from sites at the Semipalatinsk Test Site (STS), where areas with elevated levels of radioactive contamination still persist [9, 10, 11, 12]. These research findings are applicable to decontaminate radioactively contaminated soils of different origin, for example, such as peaceful nuclear blasts for industrial purposes, accidents and incidents accompanied by an excavation blast and so on. Further behavior (fractionation) of radionuclides that persists following their deposition on the soil will be defined by geochemical processes, in which the properties of radionuclides and soils play a key role [13, 14].

For the study, radioactively contaminated soils from the STS were selected, which resulted from a ground nuclear explosion- 'GNE', an excavation fusion explosion 'ETE', and excavation nuclear explosions- 'ENE-1', 'ENE-2'-(Figure 1).

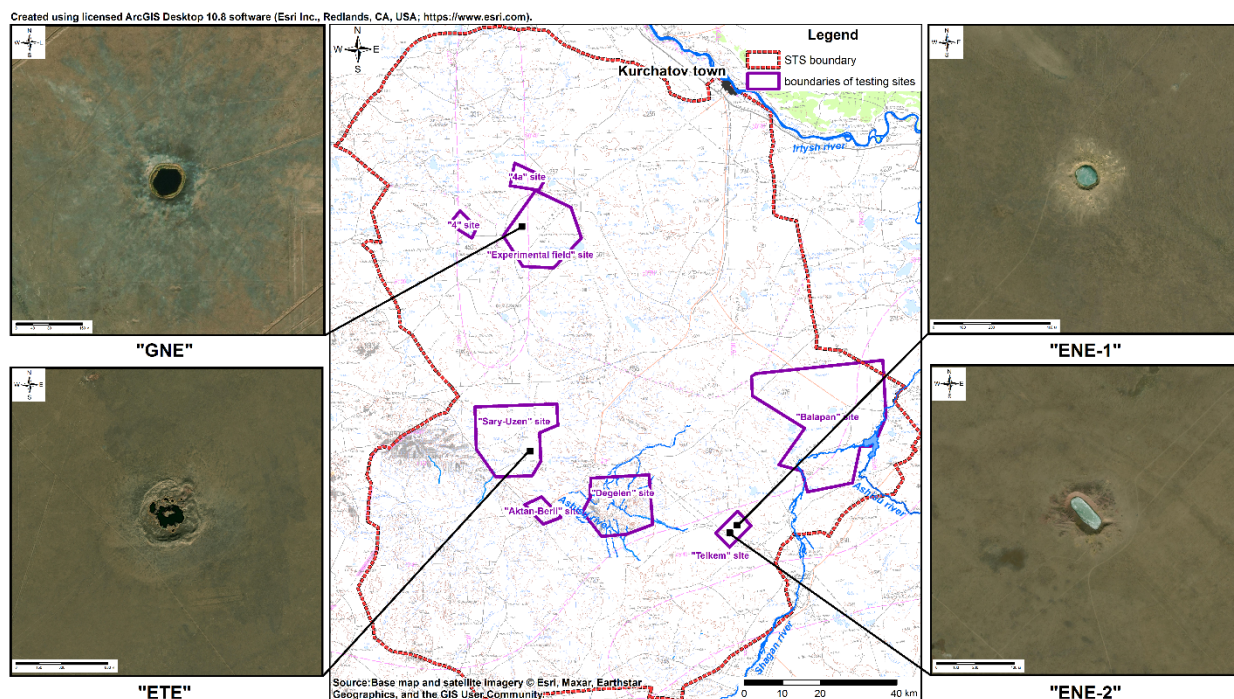


Figure 1 - Location of the objects of interest at the STS (Maps created using ArcGIS Desktop 10.8, [www.esri.com](http://www.esri.com))

The objects under study are water-filled craters of various size. 'GNE' object- warfare borehole No. 5 - represent a crater formed as a result of a ground nuclear explosion at the former 'Experimental Field' test location (no information available on the test characteristics) [15]. The maximum height of the crater rim is about 3.5 m, the total area is 102,345 m<sup>2</sup>. The volume of the crater dump reaches 7,405 m<sup>3</sup>. The crater contains water. The 'ETE' object - warfare borehole No. 101 - represent a lake formed as a result of a nuclear thermonuclear excavation explosion conducted at the former 'Sary-Uzen' test location (the yield was 0.02-0.15 kt, 12/18/1966) [16]. The perimeter of the lake is surrounded by dumps of varying height and width, composed of large blocks and rock fragments of different origin, as well as loose soil. The height of the dumps reaches an excess of 30-50 m above the plain, the diameter along the ridge of the soil dump is 520 m. 'ENE-1' and 'ENE-2' objects are located at the former 'Telkem' test location [17]. As a result of the nuclear explosion at 'ENE-1' ('Telkem-1' warfare borehole, detonation depth - 31.4 m, the yield - 0.24 kt, 10/21/1968), a regularly shaped crater (from the initial surface) of 80 m in diameter and 21 m deep was formed. The radius of the excavated soil was 110-140 m. As a result of the group nuclear explosions at 'ENE-2' ('Telkem-2' warfare borehole, detonation

depth - 31.4 m, three charges of 0.24 kt each, 11/12/1968), a trench and a dump appeared. Immediately after the explosions, the craters were filled with ground waters.

### Results and discussion

The soils of the craters under study are characterized by a high level of the activity concentrations of man-made  $^{137}\text{Cs}$  and  $^{241}\text{Am}$  and are classified as radioactively contaminated waste (RW) (Table 1) [18].

Table 1 - Activity concentration of  $^{137}\text{Cs}$  and  $^{241}\text{Am}$  in the crater soils, Bq/kg

Sampling points	Activity concentration of radionuclides, Bq/kg		Sampling points	Activity concentration of radionuclides, Bq/kg	
	$^{137}\text{Cs}$	$^{241}\text{Am}$		$^{137}\text{Cs}$	$^{241}\text{Am}$
GNE			ENE-1		
North	5700 ± 1100	1900 ± 400	North	700 ± 140	2800 ± 600
East	20000 ± 4000	1900 ± 400	East	3250 ± 650	10900 ± 1100
South	11000 ± 2000	700 ± 150	South	910 ± 185	2700 ± 550
West	17000 ± 3000	1000 ± 200	West	2200 ± 450	3500 ± 700
Min-Max	1 100 - 20 000	700 - 1 900	Min-Max	700 - 2 200	22 700 - 10 900
ETE			ENE-2		
North	190 ± 37	9.4 ± 1.8	North	1500 ± 300	4800 ± 900
East	1100 ± 200	84 ± 16	East	105 ± 20	3.6 ± 0.8
South	950 ± 185	47 ± 9	South	6400 ± 1250	17000 ± 3500
West	1500 ± 300	46 ± 9	West	8200 ± 1650	1400 ± 300
Min-Max	190 - 1 500	9.4 - 84	Min-Max	105 - 8 200	3.6 - 17 000

According to fractionation results, across all objects, most of the soil—ranging from 24% to 43% of the total mass of all fractions—is composed of particles smaller than 0.5 mm (Figure 2). At the 'ENE-2' object, a high content of fractions larger than 10 mm, from 22 to 35%, could also be noted.

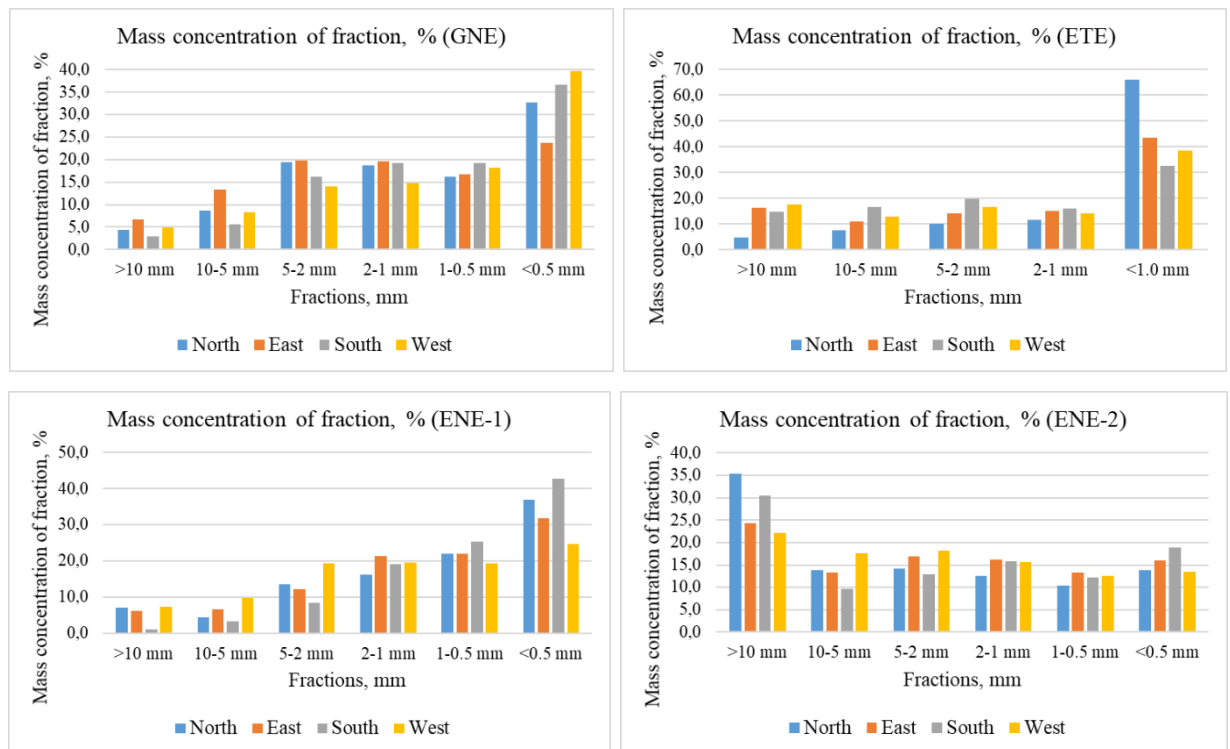


Figure 2 - Concentration ratio of particle-size fractions of the crater soils, %

The activity concentrations of  $^{137}\text{Cs}$  and  $^{241}\text{Am}$  in the selected fractions were determined. The measurements are tabulated in Table 2, denoted in figures 3 and 4.

Table 2 - Activity concentration of  $^{137}\text{Cs}$  and  $^{241}\text{Am}$  in particle-size fractions of soils, Bq/kg

Sampling points	Activity concentration of radionuclides in fractions, Bq/kg					
	>10 mm	10-5 mm	5-2 mm	2-1 mm	1-0.5 mm	<0.5 mm
<b><math>^{137}\text{Cs}</math></b>						
'GNE'						
North	590±120	2100±400	2900±600	4200±800	5200±1000	8800±1800
East	15000±3000	14000±3000	15000±3000	14000±3000	17000±3000	225000±5000
South	9600±1900	6300±1300	7500±1500	9400±1900	11000±2000	17000±3000
West	140000±30000	29000±6000	23000±5000	16000±3000	12000±2000	12000±2000
Min-Max	590-140 000	2 100-29 000	2 900-23 000	4 200-16 000	5 200-17 000	8 800-225 000
'ETE'						
North	28±6	86±17	180±40	190±40	195±40	-
East	380±80	620±120	930±190	1100±200	1600±300	-
South	140±30	370±70	620±120	880±180	1400±300	-
West	220±40	810±160	810±160	1100±200	2300±500	-
Min-Max	28-380	86-810	180-930	190-1 100	195-2 300	-
'ENE-1'						
North	220±40	340±70	300±60	410±80	830±170	1100±200

Sampling points	Activity concentration of radionuclides in fractions, Bq/kg					
	>10 mm	10-5 mm	5-2 mm	2-1 mm	1-0.5 mm	<0.5 mm
<b><sup>137</sup>Cs</b>						
East	2300±450	2500±500	2000±400	2400±500	3400±700	4400±900
South	430±90	330±70	480±100	670±130	960±190	1100±200
West	1100±200	1100±200	1600±300	2000±400	2800±600	3500±700
Min-Max	220-1 100	330-1 100	300-2 000	410-2 000	830-3 400	1 100-4 400
‘ENE-2’						
North	410±80	960±190	1300±200	1800±400	2100±400	2800±600
East	27±5	48±10	78±16	110±20	120±20	180±40
South	3000±600	5300±1000	6500±1300	6600±1300	7000±1000	8300±1700
West	1700±300	4600±900	6600±1300	8800±1800	9300±1900	14000±300
Min-Max	27-3 000	48-5 300	78-6 600	110-8 800	120-9 300	180-14 000
<b><sup>241</sup>Am</b>						
‘GNE’						
North	50±10	370±70	540±110	990±200	1500±300	3600±700
East	2000±400	1600±300	1700±300	1100±200	1100±200	1400±300
South	2100±400	750±150	690±140	520±100	530±110	710±140
West	33000±700 0	4800±1000	3500±700	1600±300	740±150	290±60
Min-Max	50-33 000	370-4 800	540-3 500	520-1 600	530-1 500	290-3 600
‘ETE’						
North	<0,6	15±3	31±6	28±6	7,1±1,4	-
East	100±20	76±15	100±20	110±20	96±19	-
South	<0,4	38±8	52±10	64±13	63±13	-
West	7,4±1,5	120±24	46±9	72±14	46±9	-
Min-Max	<0,4-100	15-120	31-100	28-110	7.1-96	-
‘ENE-1’						
North	220±40	100±20	1800±300	2000±400	3300±700	5600±1100
East	660±130	1400±200	6400±120	10000±2000	13000±300 0	14000±3000
South	530±110	510±100	2400±500	4100±800	3200±600	3700±700
West	1600±300	140±30	920±180	3200±600	5400±1100	7800±1600
Min-Max	220-1 600	100-1 400	920-6 400	2 000-10 000	3 200- 13 000	3 700-14 000
‘ENE-2’						
North	180±36	390±80	5900±1200	11000±2000	8700±1700	8300±1700
East	<0,8	<0,7	<0,8	<0,6	1,7±0,3	22±4
South	2200±400	3100±600	21000±400 0	22000±4000	20000±400 0	20000±4000
West	41±8	1800±400	2000±400	880±180	1600±300	2400±500
Min-Max	<0,8-2 200	<0,7-3 100	<0,8-21 000	<0,6-22 000	1,7-20 000	22-20 000

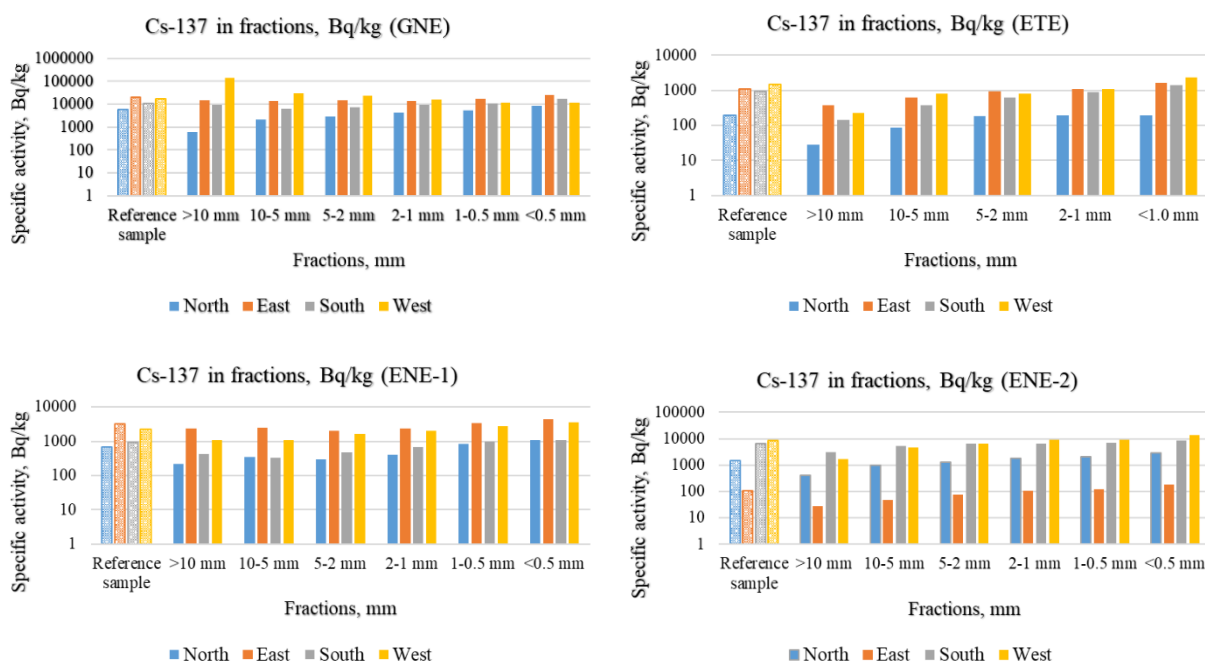


Figure 3 – Activity concentration levels of  $^{137}\text{Cs}$  in particle-size fractions of soils, Bq/kg

In the soils of the 'GNE' object formed as a result of a ground nuclear explosion, the distribution of  $^{137}\text{Cs}$  fractions is heterogeneous - the radionuclide content in fractions steadily increases as the size of one sample increases (West), with a decrease in the fraction size in the second (North). A relatively uniform distribution of the radionuclide amidst all fractions and its accumulation in the other two samples (East, South) are characterized by the smallest fractions of 1-0.5 mm and less than 0.5 mm. The 'ETE' object, formed as a result of an excavation fusion blast, and the 'ENE-1' and 'ENE-2' objects, formed as a result of excavation nuclear explosions, exhibit a gradual enrichment with  $^{137}\text{Cs}$  fractions as the particle size decreases and the maximum content of  $^{137}\text{Cs}$  in the fractions smaller than 2 mm (Figure 3). In all fractions with a peak activity concentration of  $^{137}\text{Cs}$ , its level exceeds that of the reference sample (Tables 1, 2).

In the soils of the 'GNE' object, which exceed the RW classification criterion based on the activity concentration of  $^{137}\text{Cs}$  (minimal significant specific activity (MSAC) is 10,000 Bq/kg), a decrease in MSAC of  $^{137}\text{Cs}$  in particle-size fractions was observed only in one sample (South). In this case, the radionuclide was concentrated in the smallest fractions of 1-0.5 mm and <0.5 mm, at the level of 11,000 Bq/kg and 17,000 Bq/kg, respectively. In the

remaining two samples (East and West), there is no decrease in the level of the activity concentration of  $^{137}\text{Cs}$  below the RW classification criterion.

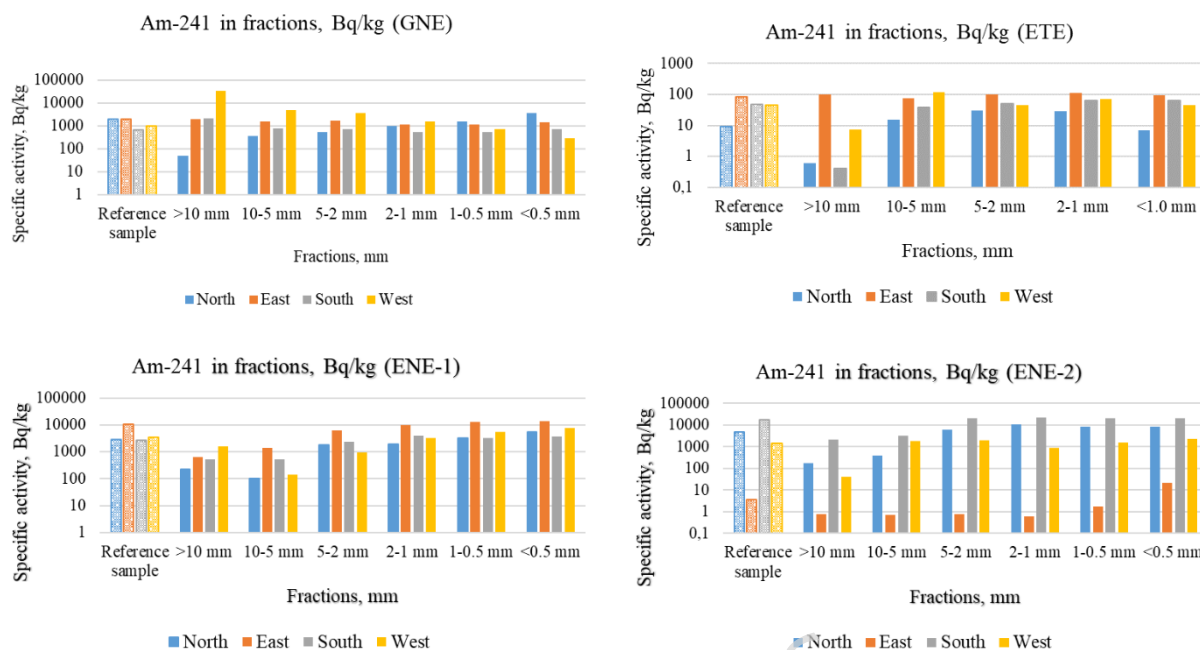


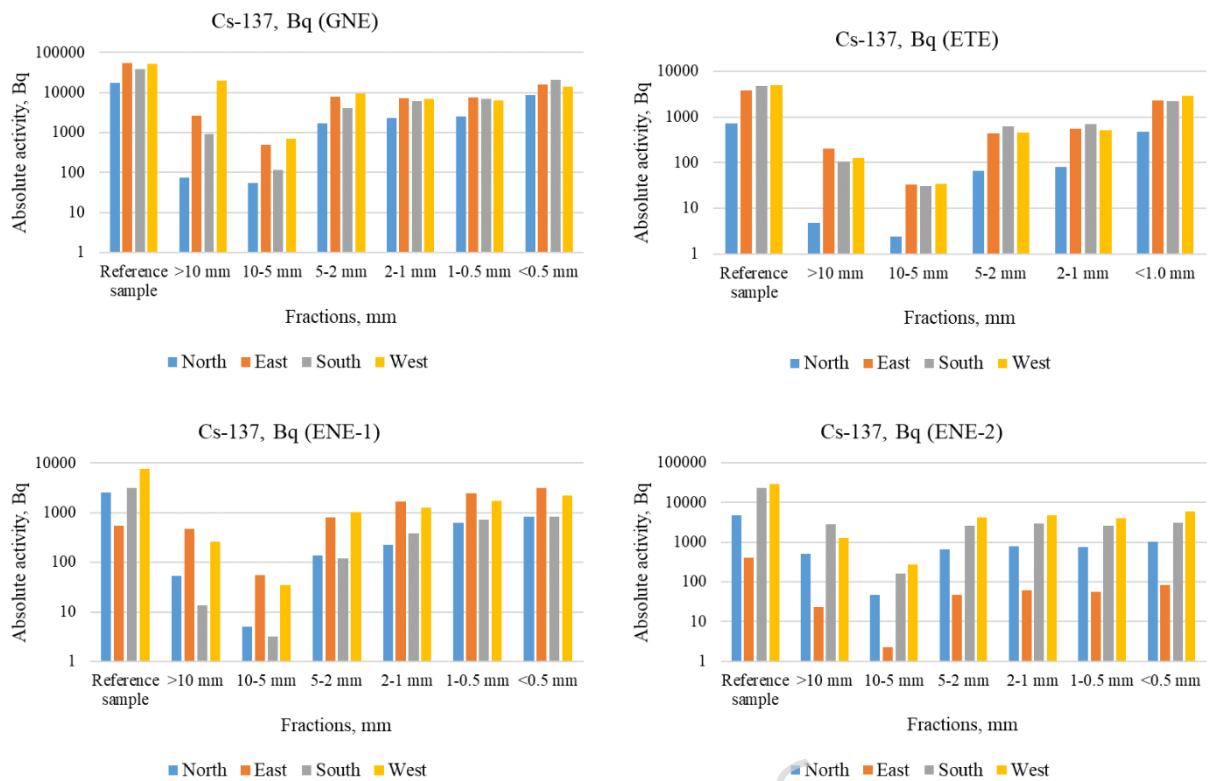
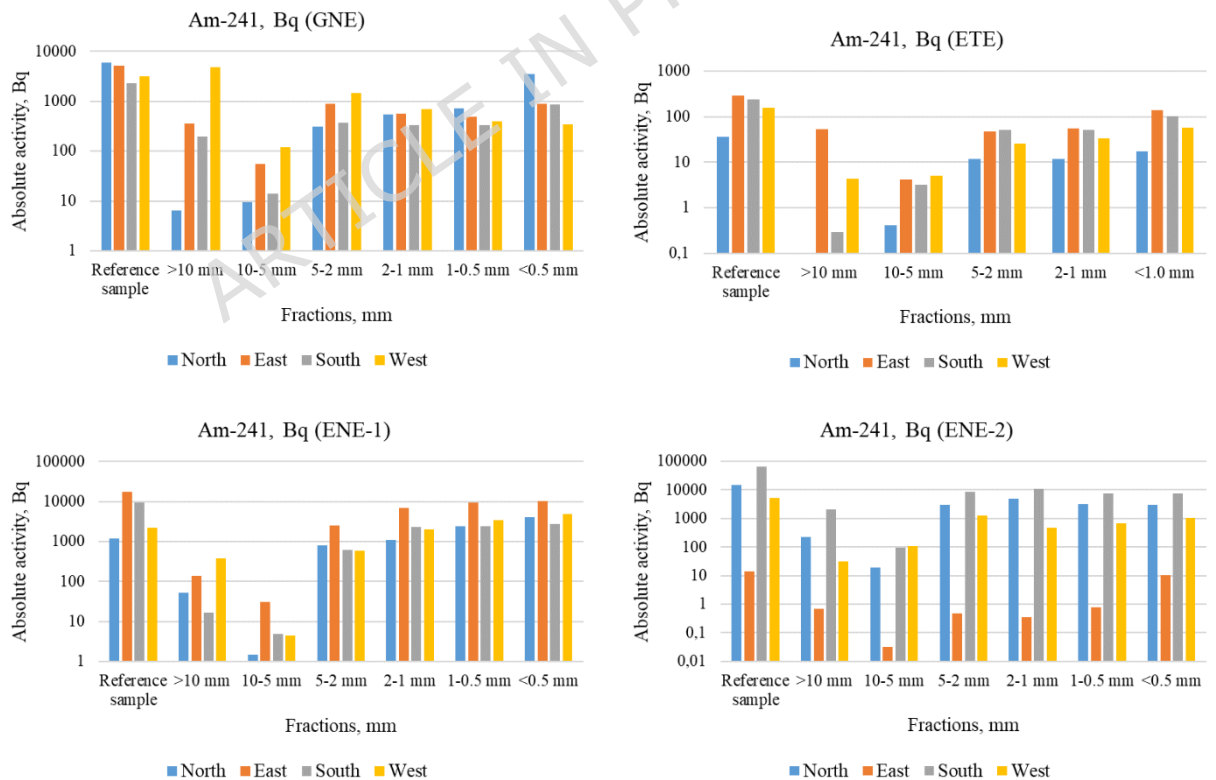
Figure 4 - Activity concentration of  $^{241}\text{Am}$  in particle-size fractions of soils, Bq/kg

At the 'GNE' object, three out of four samples (East, South, West) show  $^{241}\text{Am}$  accumulation in fractions larger than 10 mm, with a decrease in the activity concentration as a fraction size decreases. In contrast, the North sample show the opposite trend: a steady increase in  $^{241}\text{Am}$  activity with a decreasing fraction size, peaking in the fraction smaller than 1 mm.

At the 'ETE' objects, particle-size fractionation resulted in a decreased  $^{241}\text{Am}$  activity concentration in the fraction larger than 10 mm (in three out of four samples), while in the subsequent fractions, activity concentration levels remained close to the reference one. In the fourth sample (East), the activity concentration of the radionuclide remains at the same level in all fractions.

At the excavation nuclear blast objects 'ENE-1' and 'ENE-2', all samples tend to accumulate  $^{241}\text{Am}$  in small fractions. A decrease in  $^{241}\text{Am}$  activity concentration below the MSSA (1,000 Bq/kg) is mainly observed in the fractions larger than 10 and 10-5 mm.

The distribution of the absolute activities of radionuclides in fractions was considered (Figures 5 and 6).

Figure 5 – Absolute activity of  $^{137}\text{Cs}$  in particle-size fractions of soils, BqFigure 6 – Absolute activity of  $^{241}\text{Am}$  in particle-size fractions of soils, Bq

The distribution diagram of the absolute activities of  $^{137}\text{Cs}$  and  $^{241}\text{Am}$  in fractions indicate their accumulation by particles smaller than 1 mm. The absolute activities of radionuclides in fractions tend to increase as the fractions size decreases, with 5-10 cm fractions accumulating least, less often by fractions larger than 10 mm.

For soils with absolute radionuclide activity in the reference sample above the minimum detectable activity (MDA), a decrease in  $^{137}\text{Cs}$  absolute activity below RW classification criterion is observed in almost all fractions, except those smaller than 1 mm. A reduction in  $^{241}\text{Am}$  absolute activity below the MDA is mainly recorded in the fractions larger than 10 mm, 10-5 mm, and less frequently in the 5-2 mm fractions.

To assess radionuclide accumulation by fractions, the Enrichment Factor (Ef) was used—a parameter for radionuclide distribution in fractions proposed by A.Kabdyrakova [19]. It is defined as the ratio of the activity concentration of a radionuclide in a soil fraction to its activity concentration in the topsoil:

$$Ef = \frac{A_{fr}}{A_{soil}}.$$



Figure 7 -Ef of  $^{137}\text{Cs}$  and  $^{241}\text{Am}$  in particle-size fractions of soils

The diagrams of the distribution of Ef values (Figures 7) reflects best the distribution of radionuclides in soil fractions.

The distribution of  $^{137}\text{Cs}$  in soils of the objects generally shows a steady trend to increasing content in smaller fractions. The distribution pattern of  $^{241}\text{Am}$  is variable. At the 'ENE-1' and 'ENE-2' objects, accumulation of radionuclide by small fractions can be observed, though with varying intensity. At the 'GNE' object, the distribution of  $^{241}\text{Am}$  differs across cardinal points. It was not possible to identify a strict pattern at the 'ETE' object, since the fractional distribution of radionuclides differs for each sample.

### **Conclusion**

The studied efficiency of dry fractional separation has resulted in determining the optimal parameter, the Enrichment Factor (Ef), reflecting the distribution pattern of artificial radionuclides  $^{137}\text{Cs}$  and  $^{241}\text{Am}$  in soil fractions owing to nuclear explosions.

In radioactively contaminated soils formed as a result of nuclear explosions, the activity concentration of  $^{137}\text{Cs}$  was found to steadily increase with a decreasing soil fraction size. Accordingly, the highest  $^{137}\text{Cs}$  content was detected in the smallest fractions (<0.5 mm).

The distribution of  $^{241}\text{Am}$  is nonuniform. At objects of excavation nuclear explosions, small fractions tend to accumulate  $^{241}\text{Am}$ , similarly to  $^{137}\text{Cs}$ . For objects of ground nuclear blasts and excavation fusion explosions, no clear pattern in the fractional distribution of  $^{241}\text{Am}$  could be identified. The fractional distribution pattern of  $^{241}\text{Am}$  in soil can be influenced by the type of explosion and is also attributable to the features of migration in the soil, primarily driven by radionuclide physicochemical properties.

The authors assume that, with depth, the values of concentration ratio in particle-size soil fractions may vary in favor of larger ones, and no drastic differences can be expected in the radionuclide distribution pattern in particle-size fractions based upon the formation mechanisms of radioactive particles during ground and underground nuclear blasts.

The research findings suggest that fractional separation is a promising method for decontaminating cesium-contaminated soils.

## **Materials and methods**

### **Sampling**

At each site, sampling was carried out along four profiles located in the cardinal directions (North, West, South, East), extending outward from the ridge of the dump, except at object 'ENE-2', where the profiles were arranged symmetrically along the four sides of the oval-shaped crater (Figure 1). Two point samples were collected from each profile (at the ridge and in the middle of the slope). Prior to sampling, the topsoil of 10 cm, exposed to external influence, was removed, as the distribution of radionuclides in this layer may be essentially different. Then, on the cleaned surface, two consecutive soil samples were taken to a depth of 20 cm using a soil sampler (sides 10 \* 10 cm and a side height of 5 cm), positioned vertically at a 90° angle to the ground surface. The samples collected from each side of the dump were then combined into one mixed sample. The sampling depth was 20 cm, and the sampling area - 50 cm<sup>2</sup>. To avoid cross contamination, each mixed soil sample was placed in separate containers - double polyethylene bags.

### **Laboratory works**

#### ***Sample preparation and fractionation***

The preparation of soil samples began just after their transportation from the field. Soil samples were air-dried in the air or in the drying oven at 60°C. To avoid cross contamination, each sample was prepared separately using clean implements.

A particle-size composition was determined using a sieve technique from the mass content of particles of different grain-size, which is expressed as percentage with respect to the mass of a dry soil test sample. The entire volume of the soil sample underwent sieving. A standard set of sieves consisted of seven 10, 5, 2, and 1 mm sieves of a round die mesh and one 0.5 mm sieve of a common square copper mesh. A dry soil sample was previously ground in a porcelain mortar with a pestle. The sieves were mounted in the column and placed in the increasing mesh order from the tray. Soil samples were transferred in small portions to the top sieve, lidded, and screened by gently tapping with palms laterally until fully screened. Soil fractions retained on the sieves were poured from the top sieve onto the

mortar and additionally pestled, following which resieved through the same set. Screening completeness was checked by shaking each sieve above a sheet of paper. If any particles were present on the sheet, they were poured onto the next sieve. Sieving continued until no particles could be seen on the paper. Soil fractions retained after sieving on each sieve and passed to the tray were weighed. The mass of all soil fractions was summed up. The loss of soil upon sieving was spread over each fraction in proportion to their mass. Thereafter, this was done in the resulted fractions of >10; 10-5; 5-2; 2-1; 1-0.5 and <0.5 mm, other than object 'ETE', in whose soils the smallest fraction was <1 mm [20]. Thus, soil fractions of >10, 10-5, 5-2, 2-1, 1-0.5 and <0.5 mm were studied. An exception was the 'ETE' object, in whose soils the smallest fraction was <1 mm.

The utilization of a standard technique for particle-size fractionation provides for a crushing stage of particle-size fractions. This influences variation in a true particle-size composition of soil. Accordingly, the findings should be regarded as an 'upper bound' because they reflect the most possible pessimistic distribution scenario, which may potentially result from erosion or man-made processes over time, and true distribution values will not exceed them.

### ***Radionuclide analysis***

The efficiency of particle-size fractionation was evaluated for soils contaminated with gamma-emitting radionuclides  $^{137}\text{Cs}$  and  $^{241}\text{Am}$ . Gamma-spectrometric measurements were carried out using GEM FX 7025-P4 Ortec from Ametek and BE 3830 from Canberra, both equipped with high-purity germanium (HPGe) solid-state detectors with a relative detection efficiency of 35% allowing for a robust detection of gamma rays in the low-energy range [21]. For efficiency calibration, bulc volumetric sources like reference special-purpose activity measures of activity (OMACH) (Russia), RgU, RgTh, and RgK (IAEA) were used. Typical detection limits for  $^{137}\text{Cs}$  and  $^{241}\text{Am}$  were 0.1 Bq/kg.

### **Data availability**

The authors declare that the data supporting the findings of this study are available within the paper.

## References

1. INTERNATIONAL ATOMIC ENERGY AGENCY, Classification of Radioactive Waste, IAEA Safety Standards Series No. GSG-1, IAEA, Vienna (2009).
2. Sobolev A. I., SamoiloV A. A. Experience of handling radioactively contaminated soil during decommissioning of nuclear heritage facilities / A. I. Sobolev, A. A. SamoiloV // *Radioactive waste*. **1** (22), 91-101 (2023).
3. Subbotin, S.B. et al. Assessment of the radiological situation near a mothballed uranium mining facility in North-East Kazakhstan. *Scientific Reports*. **15**, 16426 (2025).
4. Volkov, V.G. et al. The experience of decontamination of radioactive soil in the territory of the Kurchatov Institute Research Center. *Atomic Energy*. **1** (110), 106-112 (2011).
5. Varlakov, A.P., Germanov, A.V. Maryakhin, M.A., Varlakova, G. A. Technology of decontamination of radioactively contaminated soil. *Analytic*. **1** (38), 46-50 (2018).
6. Israel Yu.A. Isotopic composition of fallout. L.: Gidrometeoizdat, 1973. P. 54-85
7. Nuclear explosion physics / Edited by V.M. Loborev, B.V. Zamyshlyayev, Ye.P. Maslin, B.A. Shilobreyev. M.: Nauka, Phizmatlit, 1997. Vol. 1, P. 276-281
8. Izrael, Y. A. (2545). Radioactive fallout after nuclear explosions and accidents. Elsevier. - 2002, 281 p.
9. Kunduzbayeva, A.Ye. et al. Speciation of  $^{137}\text{Cs}$ ,  $^{90}\text{Sr}$ ,  $^{241}\text{Am}$ , and  $^{239+240}\text{Pu}$  artificial radionuclides in soils at the Semipalatinsk test site. *J. Environ. Radioact*. **249(10)**, 106867 (2022).
10. Krivitskiy, P.Ye., Larionova, N.V., Baklanova, Y.V., Aidarkhanov, A.O. & Lukashenko, S.N. Characterization of areal radioactive contamination of near-surface soil at the Sary-Uzen site in the Semipalatinsk test site. *J. Environ. Radioact*. **249**, 106893 (2022).
11. Baklanova, Yu.V. et al. Comparison of  $^{90}\text{Sr}/^{137}\text{Cs}$  activity ratios in the soil of fallout plumes from aboveground nuclear and thermonuclear tests at the Semipalatinsk Test Site, 2025. *J. Environ. Radioact*. **287**, 107726 (2025).
12. Monayenko, V., Krivitskiy, P., Abisheva, M., Lukashenko, S. & Larionova, N. Determination of the geographical coordinates of the aboveground nuclear tests epicenters. *Plos One*. **19** (8), e0308920 (2024).
13. Israel Yu.A., Stukin, E.D. Gamma radiation of radioactive fallout (ed. Podoshvina, V.A.) 224 p. (Atomizdat, 1967).
14. Lavrenchik, V.N. Global precipitation of nuclear explosion products (ed. Lavrenchik, V.N.) 170 p. (Atomizdat, 1965).
15. Batyrbekov, E., Aidarkhanov, A. Vityuk, V., Larionova, N., Umarov, M. Comprehensive radioecological survey of Semipalatinsk Test Site (ed. Batyrbekov, E.) 339 p. (Kurchatov, 2021).
16. Krivitskiy, P.Y et al. Peculiarities of radioactive soil contamination in places of underground nuclear tests at the Semipalatinsk Test Site. *J. Environ. Radioact*. 253-254, 106991 (2022).

17. Larionova, N.V. et al. Transfer parameters of radionuclides from soil to plants at the area of craters produced by underground nuclear explosions at the Semipalatinsk test site. *J. Environ. Radioact.* 237(1-2), 106684 (2021).

18. Health standards of radiation safety assurance: approved by the order of the Minister of Health of the Republic of Kazakhstan dated August 2, 2022 No. KR DSM-71. (in Russ.).

19. Kabdyrakova, A.M. et al. Distribution of artificial radionuclides in particle-size fractions of soil on fallout plumes of nuclear explosions. *J. Environ. Radioact.* 186, 45-53 (2018).

20. GOST 12536-2014, 2015. Soils. Methods of Laboratory Particle-size (Grain-Size) and Microaggregate Distribution. Standartinform, Moscow (in Russian).

21. Radionuclide activity in counting samples / Measurement method on gamma-ray spectrometers using the software 'SpectraLine'. Mendeleevo: SSMC 'VNIIFTRI', 2014. Certificate of attestation No. 43151.4B207/01.00294-2010 dated 02/28/2014, 27 p.

## Legends

Figure 2 - Location of the objects of interest at the STS (Maps created using Arcgis Desktop 10.8, [www.ersi.com](http://www.ersi.com))

Figure 2 - Concentration ratio of particle-size fractions of the crater soils, %

Figure 3 - Activity concentration levels of  $^{137}\text{Cs}$  in particle-size fractions of radioactively contaminated soils, Bq/kg

Figure 4 - Activity concentration of  $^{241}\text{Am}$  in particle-size fractions of soils, Bq/kg

Figure 5 - Absolute activity of  $^{137}\text{Cs}$  in particle-size fractions of soils, Bq

Figure 6 - Absolute activity of  $^{241}\text{Am}$  in particle-size fractions of soils, Bq

Figure 7 - Ef of  $^{137}\text{Cs}$  and  $^{241}\text{Am}$  in particle-size fractions of soils

Table 3 - Activity concentration of  $^{137}\text{Cs}$  and  $^{241}\text{Am}$  in the crater soils, Bq/kg

Table 4 - Activity concentration of  $^{137}\text{Cs}$  and  $^{241}\text{Am}$  in particle-size fractions of soils, Bq/kg

## Author contributions

A. Kunduzbayeva - Conceptualization, Data Curation, Formal Analysis, Writing (Original Draft); A. Kabdyrakova - Methodology, Writing (Review & Editing); A. Mendubayev - Methodology, Data Curation; A. Panitskiy - Conceptualization, Funding Acquisition, Project Administration, Writing (Review & Editing); N. Larionova - Validation, Writing (Review & Editing); V. Baklanov - Validation, Writing (Review & Editing).

**Funding.** This research was funded by the Science Committee of the Ministry of Science and Higher Education of the Republic of Kazakhstan, grant number BR24993140 and grant number AP08856225.

**Declaration of interests.** The authors declare no competing interests.

ARTICLE IN PRESS